Pseudocobalamin production and use in *Synechococcus* cultures and communities

Catherine C. Bannon[1], Maria A. Soto[1], Elden Rowland[1], Nan Chen[1], Anna Gleason[1], Emmanuel Devered[2], Julie LaRoche[1], Erin M. Bertrand[1]*

[1]Department of Biology and Institute for Comparative Genomics, Dalhousie University, Halifax, Nova Scotia, Canada
[2]Bedford Institute of Oceanography, Fisheries and Oceans Canada, Dartmouth, Nova Scotia, Canada

*** Correspondence:**
erin.bertrand@dal.ca

Running head: psB_{12} in *Synechococcus*

Keywords: marine vitamin dynamics, methionine synthase, North Atlantic Ocean, picocyanobacteria, cobalamin

Abstract

Cobalamin influences marine microbial communities because an exogenous source is required by most eukaryotic phytoplankton, and demand can exceed supply. Pseudocobalamin, psB_{12}, is a cobalamin analog that is produced and used by most cyanobacteria but is not directly available to eukaryotic phytoplankton. A subset of microbes can remodel pseudocobalamin into cobalamin, but a scarcity of pseudocobalamin measurements impedes our ability to evaluate its importance for marine cobalamin production. Here, we perform simultaneous measurements of pseudocobalamin and methionine synthase (MetH), the key protein that uses it as a co-factor, in *Synechococcus* cultures and natural communities. In *Synechococcus* sp. WH 8102, pseudocobalamin quota decreases in low temperature (17 °C) and low N:P, while MetH did not. Pseudocobalamin and MetH quotas were influenced by culture methods (batch vs semi-continuous) and growth phase (exponential vs stationary). Despite the variability present in cultures, we found a comparably consistent quota of 296 ± 101 pseudocobalamin molecules per cyanobacterial cell in the Northwest Atlantic Ocean, suggesting that cyanobacterial cell counts may be sufficient to estimate psB_{12} inventories in this region. This work offers insights into cellular pseudocobalamin metabolism and the environmental and physiological conditions that may influence it and provides environmental measurements to further our understanding of when and how pseudocobalamin can influence marine microbial communities.

Introduction

Cobalamin, B_{12}, is an essential organic micronutrient that impacts microbial community composition and productivity in various parts of the ocean (Koch *et al.*, 2011; Bertrand *et al.*, 2015). Most cyanobacteria produce and use a unique cobalamin analog called pseudocobalamin, psB_{12}, that is poorly bioavailable to most eukaryotic phytoplankton because of its structural differences at the α-ligand (adenine = psB_{12}, DMB = B_{12}) (Helliwell *et al.*, 2016; Heal *et al.*, 2017). Similar to B_{12}, psB_{12} occurs in different forms (Me-, Ado- and OH-psB_{12}), which have unique functions in the cell (Fig 1A). psB_{12} has the potential to impact B_{12} availability through the activities of remodelers, such as select heterotrophic bacteria and eukaryotic algae, which are able to exchange the adenine α-ligand for DMB (Helliwell *et al.*, 2016; Ma *et al.*, 2020). The prevalence of and controls on psB_{12} production and use remains unclear, in part due to the limited measurements of psB_{12} in cultures and in the natural environment.

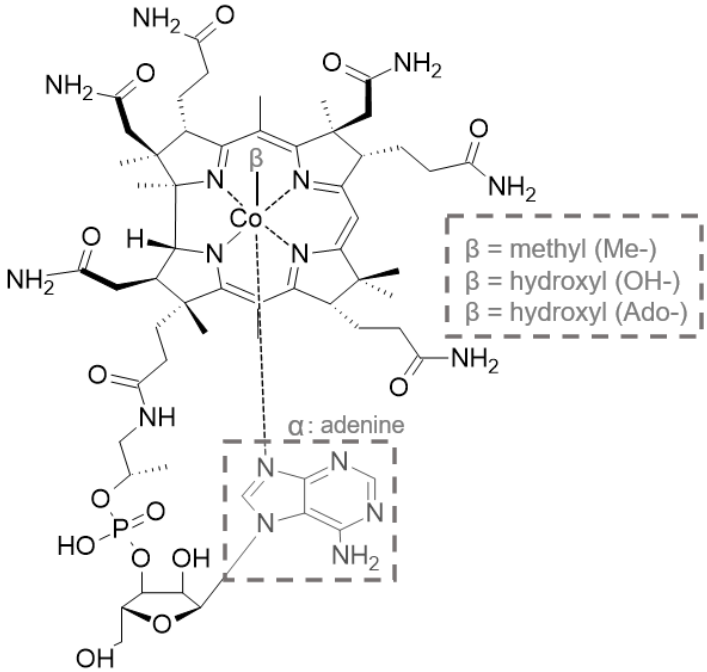

Figure 1: Structure of pseudocobalamin, psB_{12}, with adenine at the alpha (α) ligand and Me-, OH- or Ado- at the beta (β) ligand. C:N ratios of the molecules are as follows (OH-psB_{12} = 3.6:1, Me-psB_{12} = 3.6:1, Ado-psB_{12} = 3.2:1).

Accurately quantifying metabolites can help characterize the composition, activity, and controlling processes in marine microbial communities. However, such measurements remain difficult in part because of the complex and unknown chemical backgrounds they are embedded in (Kido Soule *et al.*, 2015; Moran *et al.*, 2022). Multiple studies have quantified particulate cobalamin, while only one study to date has quantified particulate psB_{12} in the ocean (Heal *et al.*, 2017). Concentrations of particulate psB_{12} ranged from undetectable to 0.15 pM. These values correlated with cyanobacterial carbon and co-occurred with B_{12} (Heal *et al.*, 2017). Quantifying both psB_{12} and B_{12} compounds would provide a more complete picture of the processes governing cobalamin availability, especially in regions vulnerable to cobalamin co-limitation and where cyanobacteria are abundant.

Insight into psB_{12} cell biology is restricted because psB_{12} quotas have only been quantified to date in four cyanobacterial strains (Heal *et al.*, 2017) and the influence specific biotic or abiotic factors have on psB_{12} production and use have yet to be explored, either in culture or in the field. One key psB_{12}-dependent enzyme in cyanobacteria is methionine synthase (MetH or MS), which requires *methyl*-psB_{12} (Me-psB_{12}) as a cofactor to generate methionine from homocysteine and 5-methyltrahydrofolate (Tanioka *et al.*, 2009, 2010; Heal *et al.*, 2017). Some cyanobacteria also encode NrdJ, a class II ribonucleotide reductase that is expected to use Ado-psB_{12} to generate dNTPs from their ribonucleotide metabolites through a deoxygenation step (Gleason and Olszewski, 2002; Lundin *et al.*, 2010), though the use of psB_{12} by this enzyme has yet to be specifically examined . The psB_{12} biosynthesis pathway includes up to 30 enzymes (Cob/Cbi proteins) and represents a great energetic and genomic cost, but the specific bottleneck or rate limiting step of this pathway remains unclear (Rodionov *et al.*, 2003; Lu *et al.*, 2020). Quantifying proteins involved in both psB_{12} production and use has the potential to provide mechanistic details into psB_{12} cell biology but has thus far not been investigated.

Synechococcus is one of the most abundant cyanobacterial genera in the ocean (Flombaum *et al.*, 2013), and thus is likely to be a major source of psB_{12}. In particular, *Synechococcus* is an important member to the microbial community in the Northwest Atlantic Ocean in coastal euphotic zone waters during the fall (Li and Wood, 1988; Zorz *et al.*, 2019; Robicheau *et al.*, 2022; Soto *et al.*, 2023). Environmental trends in this region indicate that the plankton community is subject to large changes in temperature and nitrogen availability (Loder *et al.*, 2013). Investigating the influence these factors have on *Synechococcus* psB_{12} activity could provide insight into how the psB_{12} inventory may fluctuate in this region.

Here, we leverage targeted metabolomics and proteomics to investigate psB_{12} production and use in *Synechococcus* cultures and in communities from the Northwest Atlantic Ocean (NWA). We cultured *Synechococcus* sp. WH 8102 under a range of abiotic (low N:P, low temperature), biotic (diel cycle, growth phase) and distinct culture conditions (batch culture, semicontinuous culture). By measuring both psB_{12} production and use in these conditions, we obtain quantitative insights into *Synechococcus* psB_{12} cell biology while constraining psB_{12} quotas and highlighting environmental and physiological conditions that may impact it. Then, using samples collected from the NWA, we investigate in situ psB_{12} quotas and use in environmental *Synechococcus* communities through protein and co-factor quantification.

Material and methods

Identification of proteins and selection of peptides

We performed a literature search to identify proteins involved in psB_{12} production (Cob/Cbi proteins) and utilization (MetH and NrdJ). BLASTp was used to search for homologues of these *Synechococcus* sp. WH 8102 proteins in other available marine *Synechococcus* genomes using the GenBank nr database. Proteins were aligned using COBALT (Papadopoulos and Agarwala, 2007) and digested in silico with trypsin to reveal conserved peptides. Sequences were introduced in the Unipept Tryptic Peptide Analysis search (Gurdeep Singh *et al.*, 2019) to determine if the peptide is present in a significant number of the *Synechococcus* strains of interest. Peptides for CobO (psB_{12} production) and MetH (psB_{12} use) were selected for analyses as they met the peptide selection guidelines for SRM targeted assays described in Hoofnagle et al. (2016) (Hoofnagle *et al.*, 2016). Peptides are reported in Table S1. We found no suitable peptide with adequate coverage across *Synechococcus* clades for NrdJ.

Culture experiments to measure *Synechococcus* peptides and pseudocobalamin quotas

Synechococcus sp. WH 8102 (CCMP2370) obtained from the National Center for Marine Algae and Microbiota (NCMA, Bigelow Laboratory, USA) was maintained axenically in modified Synthetic Ocean Water (SOW) media, void of CN-B_{12}, under ~20 µmol photosynthetically active radiation m^{-2} s^{-1} in a light:dark cycle of 12:12 h unless otherwise described (Table 1). Throughout culturing, we monitored growth via relative fluorescence units (RFU) measured in a 10-AU Fluorometer (Turner Designs, San Jose, CA), and cell counts using a BD Accuri™ C6 flow cytometer as described below. Cultures were also tested for axenicity once a week using SYBR Green II dye (Invitrogen) followed by flow cytometry screening. Specific growth rates (d^{-1}) were calculated using linear regression of ln RFU during exponential growth.

We maintained semicontinuous cultures of WH 8102 in exponential phase by replacing a volume of culture with fresh media to dilute the cell concentration to a fixed value every other day (Table 1). Semicontinuous cultures were grown in three conditions, control (24±1 ºC; 26 N:P), low temperature (17±1 ºC; 26 N:P) and low N:P ratio (24±1 ºC;10 N:P) (Fig S1). Cultures (n=3) were maintained for ~7 generations in exponential phase under the conditions described before harvesting. We harvested protein samples (50 mL) on 0.2 µm polycarbonate filters, metabolite samples (50 mL) on 0.2 µm Nylon filters, and particulate organic carbon (POC) samples (20 mL) on GF/F glass microfiber filters.

Table 1: Experimental treatments (n=3) performed on *Synechococcus* sp. WH 8102 in specific culture methods.

Treatment	Culture methods	Harvesting time
Control (24±1 ºC; 26 N:P)	Semicontinuous	after ~7 generations (Exponential phase)
Low temperature (17±1 ºC)		
Low N:P ratio (10 N:P)		
Diel cycle (harvest at 9:30, 18:00 and 22:00)	Batch	Exponential phase
		Stationary phase

For strain WH 8102 grown in batch culture, we harvested samples at both exponential and stationary phase (Fig S1). For early exponential phase, we harvested 35 mL for protein samples, 17 mL for metabolite samples, and 8 mL for POC samples at the three points in the diel cycle. In stationary phase, we harvested 20 mL for protein samples, 10 mL for metabolite samples, and 5 mL for POC samples at the three points in the diel cycle. The three points of the

diel cycle evaluated were: 1.5 hours after the lights went on (9:30), 1 hour before the lights went off (18:00), and 3 hours after the lights went off (22:00).

Cyanobacterial culture cell counts

Culture cell density was measured on an Accuri C6 flow cytometer (BD) after labeling with1:1000 SYBR Green II dye (Invitrogen). Single cell events were recorded on forward side scatter and side scatter plots and distinguished using FL2-A (PE) (Phycoreythrin, ex: 488 nm) and FL32A (Chl *a*) (Chlorophyll *a,b,* ex = 488 nm, rm > 640 nm). Accuri run limits were set to a maximum of 500,000 events or 50 µL, with a fluidics speed of 35 µL/min at a core size of 16 µm. The gating strategy for *Synechoccus* populations was developed based on the Acccuri application note provided by BD Biosciences.

POC Measurements

Samples were acidified for 6 hours in a glass desiccator with an open bottle of concentrated hydrochloric acid and later dried overnight at 45 °C. Filters were packed in tin capsules and analyzed for particulate carbon on an elemental analyzer (Elementar Vario microcube) coupled to an IRMS (Isoprime 100). The samples were flash combusted at 1150 °C to convert particulate carbon into CO_2 gas. These gaseous components were then analyzed by the Isoprime 100. The values were blank-corrected and divided by cell number to give per cell quota.

Environmental Sample Collection

We collected environmental samples in Fall 2016 onboard an AZMP (Atlantic Zone Monitoring Program) cruise aboard CCGS Hudson from September 15th, 2016, to October 6th, 2016 (HUDSON 2016027). Samples were taken at 4 stations on the Halifax line (HL 01, HL 02, HL 05.5, HL 06) (Table S2). At each of the stations, we collected 1 L of water at each depth for particulate metabolite analysis. The sample was gently filtered through a 0.2 µm Nylon filter in the dark to reduce photodegradation. For protein samples, 10 L of water was pre-filtered (330 µm) from Niskin bottles then filtered gentled through 3 and 0.2 µm polycarbonate filters via peristaltic pumping. Parallel 1.8 mL seawater samples for analytical flow cytometry were fixed with 1% paraformaldehyde. Flow cytometry samples and filters were then frozen immediately at -80°C until analysis.

Particulate metabolites extraction

Metabolites were extracted from both culture and environmental samples following the methodology described by Heal et al. (2017) with minor modifications. Heavy-CN-B_{12} (Cambridge Isotopes Labs, CLM-9770-E) was used as an internal standard and was added to a final concentration of 3 nM in all metabolite samples prior to extraction. Briefly, metabolites were extracted using an organic solvent extraction paired with bead beating. Solvent was removed under vacuum (Eppendorf, Mississauga, ON) at room temperature. Culture samples were re-suspended in buffer A (20 mM ammonium formate, 0.1% formic acid, 2% acetonitrile) to generate equivalent of extracts from 12,100 cells/µL. Environmental samples were resuspended with 100 µL of buffer A. All samples were then vortexed and centrifuged at 10,000 x g for 3 min at 4 ºC and then diluted 2-fold with buffer in conical polypropylene HPLC vials (Phenomenex, Torrance, CA) prior to mass spectrometry analysis.

Metabolite quantification

HPLC-MS was used to quantify cobalamins using a Dionex Ultimate-3000 LC system coupled to the electrospray ionization source of a TSQ Quantiva triple-stage quadrupole mass spectrometer in SRM mode. Details of mass spectrometery conditions are reported in supplement methods and the transition list is reported in Table S3.

For metabolite samples, quality control (QC) samples were prepared by mixing equal

179 volumes of each sample within its respective group (1 QC for culture samples and 1 QC for
180 environmental samples). Calibration curves with authentic cobalamin standards were prepared
181 using the QC sample as a matrix and triplicate injections were performed for 0, 0.1, 5, 10, 50,
182 and 100 fmol of each authentic cobalamin standard on analytical column with linearity up to
183 1000 fmol. All cobalamins were normalized by heavy-CN-B_{12} internal standard to account for
184 variability introduced by matrix effects, during extraction and instrument analysis. Limits of
185 quantitation and limits of detection were calculated as 10x and 3x the variation in the QC
186 sample without spike, respectively and recorded in Table S4.
187 Given that commercial psB_{12} standards are not available, the following assumptions
188 were made for psB_{12} quantification using associated cobalamin analog standards: (1) B_{12} and
189 psB_{12} ionize with the same efficiency, (2) B_{12} and psB_{12} fragments are generated in a similar
190 fashion, (3) B_{12} and psB_{12}'s different elution times do not greatly affect the response.

191 **Protein extraction and digestion**

192 Protein sample filters were submerged in 750 µL of SDS extraction buffer (2% SDS, 0.1
193 M Tris/HCl pH 7.5, 5% glycerol, 5 mM EDTA) and incubated for 10 min on ice before being
194 heated for 15 min at 95 ºC in a ThermoMixer C (Eppendorf, Mississauga, ON) at 350 RPM.
195 Samples were then sonicated on ice for 1 min with a Q125 Sonicator (Qsonica Sonicators,
196 Newton, CT) at 50% amplitude and 125 W (pulse 15 s ON, 15 s OFF) then kept at room
197 temperature for 30 min and vortexed every 10 min. The filter was then removed, and samples
198 were centrifuged at 15,000 x g for 30 min at room temperature. 4x volume of ice-cold acetone
199 was added to the supernatant for overnight precipitation of proteins at -20 ºC before washing
200 with 3 x 400 µL of ice-cold acetone and 1 x 400 µL with ice-cold methanol. Following each
201 wash, samples were centrifuged at 15,000 x g for 30 min at room temperature and the
202 supernatant was removed. Pellet was dried down under vacuum (Eppendorf, Mississauga, ON)
203 for 15 min at room temperature. Extracted protein was resuspended in 20 µL of 8 M urea for 10
204 min at room temperature then80 µL of freshly made 50 mM ammonium bicarbonate was
205 gradually added to get a final solution of 1.6 M urea and 40 mM ammonium bicarbonate.
206 Aliquots of 50 µg of protein were removed from each sample and diluted to 100 µL with
207 50 mM ammonium bicarbonate for protein digestion. Proteins were reduced with 5mM
208 dithiothreitol (DTT) at 56 ºC for 30 min in a ThermoMixer, then alkylated with 15 mM
209 iodoacetamide at room temperature in the dark. Residual iodoacetamide was quenched with a
210 second addition of DTT to give a final concentration of 10 mM DTT. Protein was digested with 1
211 µg trypsin (Thermo Scientific, Waltham, MA) at 37 ºC overnight. 0.5 µL of formic acid was added
212 to halt the digestion. A peptide BCA (Thermo Scientific, Waltham, MA) ok!was conducted to
213 confirm protein concentration of each sample before injection.

214 **Peptide quantification**

215 Targeted mass spectrometry was performed using a Dionex Ultimate 3000 UPLC system
216 interfaced to a TSQ Quantiva triple-stage quadrupole mass spectrometer (MS) (Thermo
217 Scientific, Waltham, MA), fitted with a heated, low flow capillary ESI probe (HESI-II). Isotopically
218 labeled, heavy internal standard versions of each peptide were synthesized by Thermo
219 Scientific™ at >95% purity. Heavy peptide standard was added to samples to yield 20 fmol on
220 column for every 1 ug total protein injected. Details of mass spectrometer conditions are
221 reported in supplement methods. Each sample was analyzed via triplicate injections using the
222 transition list of peptides that is found in Table S1.

223 **Environmental cyanobacterial cell counts**

224 Preserved samples were thawed at room temperature, and prefiltered using 35 µm cell
225 strainers into a 5 mL fluorescence-activated Cell Sorting (FACS) tube. The samples were then
226 collected and analyzed on a Novocyte 3000 with NovoExpress software (Agilent, USA) for
227 natural fluorescence cell counts. The Novocyte 3000 is equipped with three lasers [Red (640

nm), Blue (488 nm), and Violet (405 nm)], and the optical filters of interest are chlorophyll/phycocyanin (675/30 nm), phycoerythrin (572/28 nm), and divinyl chlorophyll a (675/30 nm). The samples were collected with a flow rate of 120 µL/min and a threshold of chlorophyll > 450 nm. The gating strategy was developed based on the Novocyte application note provided by Agilent and the *Prochlorococcus* gate was constructed with the aid of pure *Prochlorococcus* culture.

Statistical analysis

Statistical analyses were performed using R (RStudio Team, 2020). A one-way ANOVA followed by a Post-hoc Tuckey's Test was used to determine the differences in *Synechococcus* culture experiments. A two-way ANOVA followed by a Post-hoc Tuckey's Test was used to determine the effects of growth phase and diel cycle on the same variables. Differences were considered significant when a p-value < 0.05 was observed.

Results

Factors that influence psB$_{12}$ production and use in *Synechococcus* sp. WH 8102

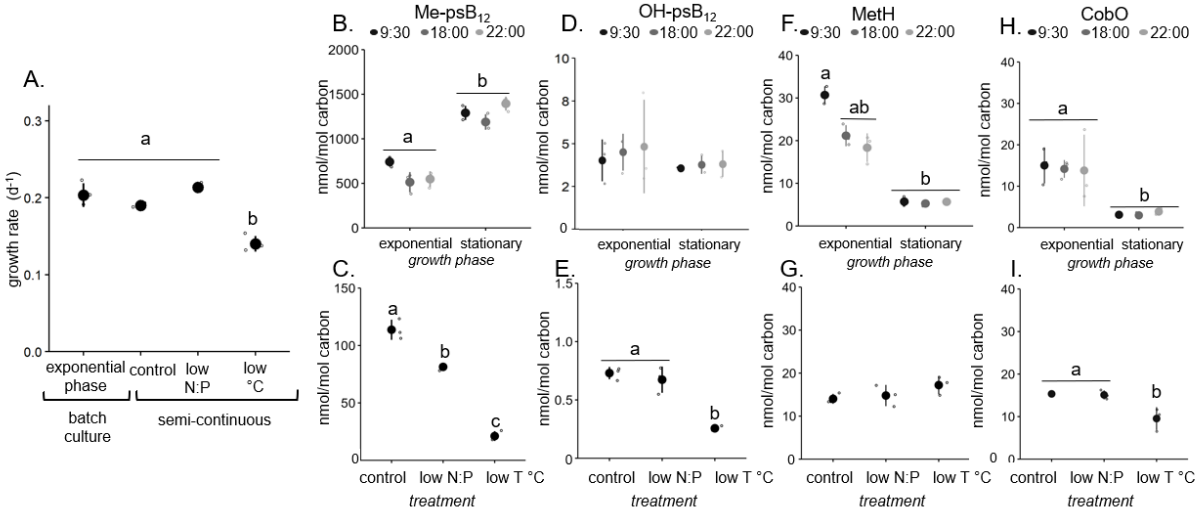

Figure 2: Changes in (A) growth rate (per day), methyl- (B, C), hydroxy- (D, E) pseudocobalamin and MetH (F, G) and CobO (H, I) (nmol per mol carbon) in *Synechococcus* sp. WH 8102 under different experimental treatments grown in batch (B, D, F, H) and in semi-continuous cultures (C, E, G, I). Mean values are represented by solid circles, individual biological replicate (n=3) values by small open circles, and the standard deviation by vertical lines. Different letters over data points indicate statistically significant differences (p-value < 0.05) between pairs of means based on the post-hoc Tukey's Test. Shared letters (i.e., a, b, c) indicate no significant difference, if no letters are displayed then the differences between treatments were insignificant.

We performed culture experiments with *Synechococcus* sp. WH 8102 in triplicate (n=3) to investigate the influence different conditions have on psB$_{12}$ production and use. Growth rates (per day) were similar to those reported in literature and were consistent across batch grown cultures and semi-continuously grown cultures in control and low nitrogen treatments but significantly lower in low temperature (17°C) (Fig 2A) (Dupont *et al.*, 2012). Mol carbon per *Synechococcus* cell increased during the day and in stationary phase, and significantly increased in low temperatures (Fig S2A, B). Microgram (µg) protein per *Synechococcus* cell was invariant across the time of day and growth phase, but significantly increased in low temperature compared to other treatments (Fig S2C, D).

Cellular Me-psB$_{12}$ quota ranged from 20 to 1500 nmol psB$_{12}$ per mol C (Fig 2B, C) and 340 to 16,000 Me-psB$_{12}$ molecules per cell (Figure S4). OH-psB$_{12}$ quota ranged from 7 to <1 nmol psB$_{12}$ per mol C in all samples, 4 to 67 molecules per cell, and accounted for <1% of total psB$_{12}$ inventory per cell (Fig 2B-E). Despite our low limit of detection (LOD) (22 molecules per cell, Table S4), we did not detect Ado-psB$_{12}$. Me-psB$_{12}$ quota did not differ across diel cycle but was significantly higher in stationary phase (Fig 2B). Both Me-psB$_{12}$ and OH-psB$_{12}$ quotas increased >350% in cultures grown in batch compared to the control cultures grown semi-continuously although there was no difference in growth rate (Fig 2B-E). For semi-continuously grown cultures, Me-psB$_{12}$ cellular quota significantly decreases at 17 °C compared to 24 °C, and when grown at 10 N:P versus the 26 N:P control (Fig 2C). In contrast, we found that OH-psB$_{12}$ quota did not increase in stationary phase and was only significantly lower when grown semi-continuously at 17 °C (Fig 2D-E).

MetH peptide concentration ranged from 5 to 33 nmol per mol C in conditions tested (Fig 2F-G), representing 0.07 to 0.18% of total cellular protein (supplemental methods), and 40 to 370 MetH copies per cell. MetH peptide concentration increased in the morning (9:30) at exponential phase when compared samples taken in the afternoon (18:00) and evening (22:00) (Fig 2F). MetH abundance (fmol per nmol carbon) did not vary in low temperature and low nitrogen. CobO concentration ranged from 3 to 24 nmol per mol C in conditions tested (Fig 2H-I), representing a 0.006 to 0.02% of total cellular protein (supplemental methods), and 20 to 240 CobO copies per cell. CobO concentration was higher in exponential phase than stationary phase and were significantly lower in cultures grown in low temperature. CobO fmol per µg protein was invariant in the conditions tested (Fig S3H, I).

psB_{12} production and use by *Synechococcus* in the Northwest Atlantic Ocean

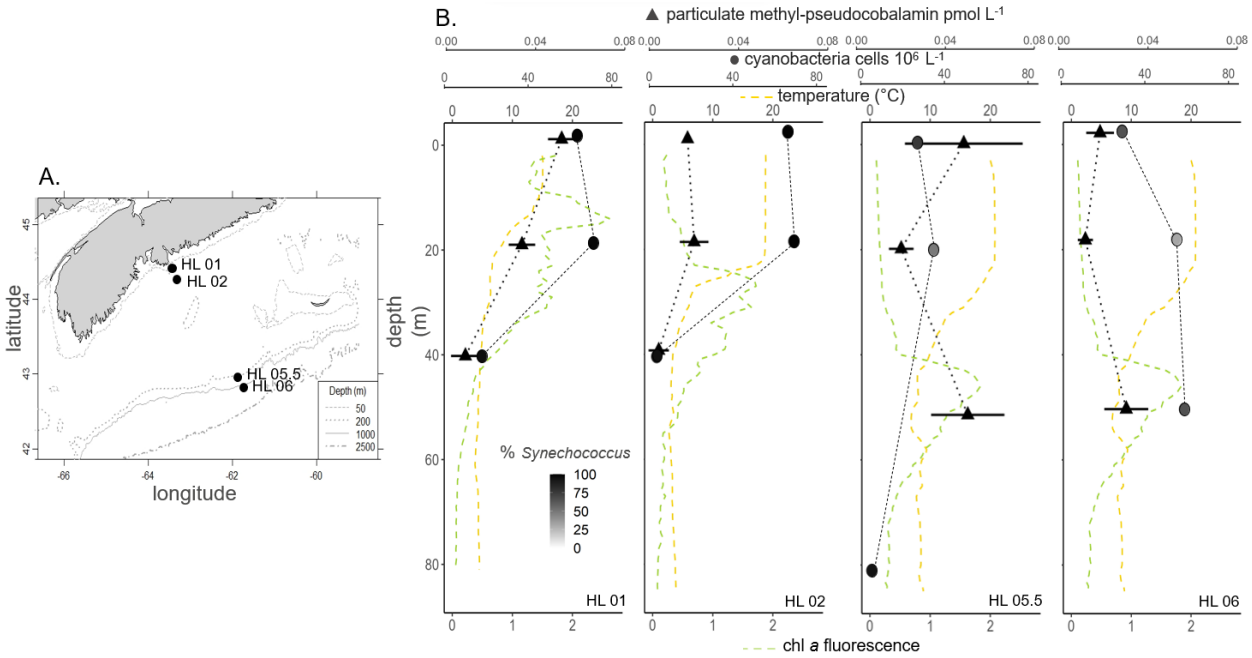

Figure 3: (A) Location of sampling on the Scotian Shelf and (B) depth profiles of particulate methyl-psB_{12} (pM, triangle), cyanobacterial abundance (10^6 cells per L, circles), temperature (°C, yellow) and chlorophyll *a* fluorescence (green) depth profiles in the Fall, 2016. For pseudocobalamin, error bar represents technical replicates of mass spectrometry measurements. Circles are shaded based on the calculated % population of *Synechococcus* cells amongst all cyanobacteria (*Synechococcus* plus *Prochlorococcus*) determined through flow cytometry.

To investigate psB_{12} production and use in the Northwest Atlantic Ocean, we measured cyanobacterial cells and particulate psB_{12} concentrations at four stations on the Scotian Shelf (HL 01, 02) and Slope (HL 05.5, 06) (Fig 3A). Peak chlorophyll *a* fluorescence (green) was between 10-30 m for HL 01 and HL 02 stations but were below 40 m for HL 05.5 and HL 06. Temperature decreased with depth at all stations but increased in surface waters from coastal to shelf break stations. Additional environmental data is provided in Table S2.

Me-psB_{12} was the only quantifiable particulate psB_{12} form, despite our method's low limits of detection for both OH- and Ado-psB_{12} (Table S4). Me-psB_{12} measurements were up to 0.08 pM and were undetectable below 50 m depth (Fig 3B). We found a higher particulate psB_{12} concentration at shallow depths and coastal waters, which generally mirrored cyanobacterial

distribution. We also measured particulate B_{12} which ranged from undetectable to 0.4 pM total, with Me-B_{12}, Ado-B_{12}, and OH-B_{12} dominant in that order (Table S2).

Synechococcus cells per L were highest in the surface at HL 01 and HL 02. *Synechococcus* dominated cyanobacterial communities in most samples except for HL 06 at 20 m and 50 m (32% and 65% respectively) where *Prochlorococcus* also contributed (Table S2). *Synechococcus* comprised >65% of the cyanobacterial community in 1 m samples from all stations and these samples were therefore chosen to be screened for the *Synechococcus*-specific MetH peptide.

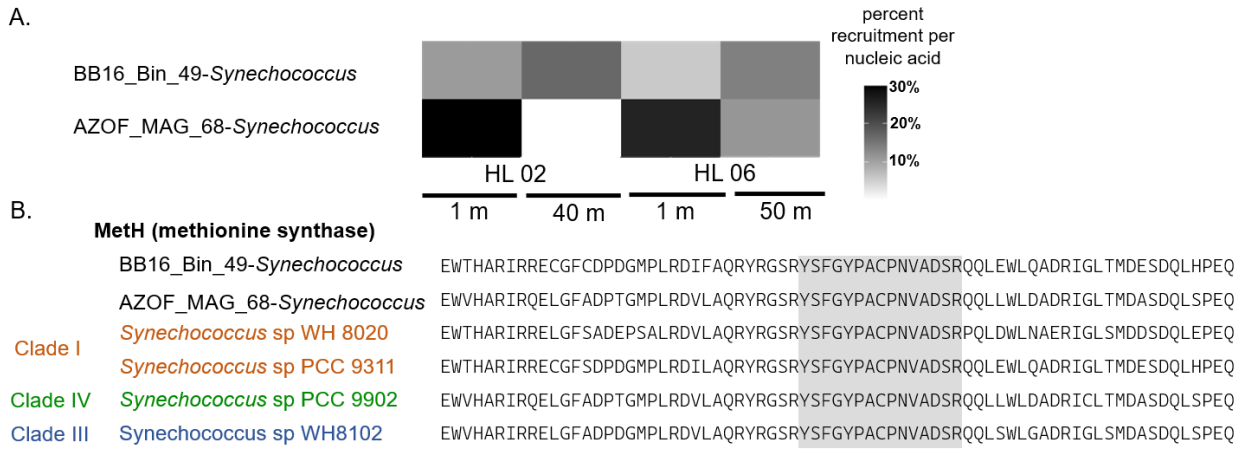

Figure 4: Assessing MetH peptide coverage in Scotian Shelf *Synechococcus* communities. (A) Recruitment of cobalamin-related reads per nucleic acid by two dominant *Synechococcus* metagenome assembled bins, shown as a proportion of all cobalamin-associated reads from the entire 0.2 um prokaryotic community at HL 02, HL 06 in Northwest Atlantic Ocean in Fall, 2016 (see Soto et al, 2023). (B) Alignment of MetH protein sequences from the two dominant assembled *Synechococcus* genome bins from Halifax Line in Fall 2016 (black) and representative *Synechococcus* genomes from Clade I (orange), Clade III (blue), Clade IV (green). Peptide used to quantify *Synechococcus* MetH in this study is highlighted in grey.

We examined the presence of the MetH peptide in environmental *Synechococcus* communities, leveraging a previous metagenomics study (Soto *et al.*, 2023). Two *Synechococcus* genome bins (BB16_Bin_49-*Synechoccus* and AZOF_MAG_68-*Synechoccus*) are present at surface depths at HL 02 and HL 06 in Fall 2016 (Soto *et al.*, 2023) (Fig 4A). The peptide we used to quantify MetH in *Synechococcus* in this study, highlighted in gray, is present in these bins. It is also present within available marine *Synechococcus* genomes from clade I, IV and III (including WH 8102), which are expected to be major *Synechococcus* clades present on the Scotian Shelf and Slope (Robicheau *et al.*, 2022) (Fig 4B). The high contribution of cobalamin-associated reads from these two dominant *Synechococcus* bins at HL 02 and HL 06 in Fall 2016, and the presence of the MetH peptide in these bins, suggests that the MetH peptide we used in this study is likely to capture the majority of *Synechococcus* MetH present in these locations.

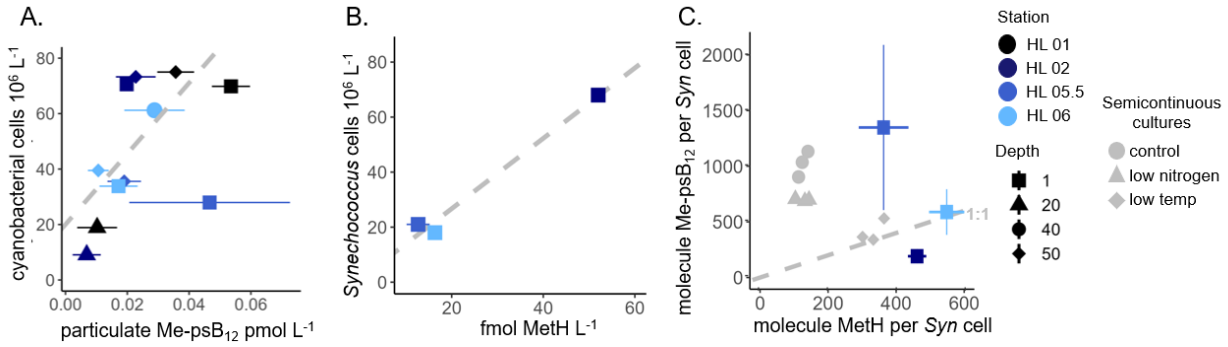

Figure 5: Pseudocobalamin production and use in the Northwest Atlantic Ocean. Relationship between (A) particulate psB$_{12}$ (pM) and cyanobacterial cell counts (10^6 L^{-1}) in environmental samples. (B) Correlation between *Synechococcus* cell (10^6 L^{-1}) and *Synechococcus* MetH abundance (fmol L^{-1}) in the surface ocean, (C) Protein (MetH) to cofactor (Me-psB$_{12}$) ratio per *Synechococcus* cell in semicontinuous culture studies (grey circle, triangle, diamond) and environmental samples (blue squares). Horizontal and vertical error bars represent technical replicates measured using LC-MS/MS.

Assuming that all Me-psB$_{12}$ originates from cyanobacteria, cyanobacteria in our samples had a Me-psB$_{12}$ quota of 296 ± 101 molecules Me-psB$_{12}$ per cell, with the exception of HL 05.5 at 1 m where there was ~1150 Me-psB$_{12}$ molecules per cyanobacterial cell (Fig 5A). Cyanobacterial cells count was used in place of *Synechococcus* cell counts as *Prochlorococcus* contributed to the cyanobacterial community in some of these samples (i.e. HL 06, Fig 3B). All *in situ* quotas fall into a range set by culture studies (Fig 2B, C). We also found an average of 460 ± 75 molecules of MetH per *Synechococcus* cell in surface samples measured (Fig 5B).

We then investigated the MetH:Me-psB$_{12}$ stoichiometry in our culture and environmental community samples. Stoichiometry allows us to determine the proportion of Me-psB$_{12}$ quota that is theoretically being used by MetH and provides insights into the *in situ* psB$_{12}$ related status of the community and how it compared to cultures. Crystal structures of MetH have revealed that there is a 1:1 MetH to Me-B$_{12}$ stoichiometry, and that MetH exclusively uses one Me-B$_{12}$ molecule as a co-factor (Matthews *et al.*, 2008; Koutmos *et al.*, 2009). Although the structure has not been explicitly determined for cyanobacterial MetH, a study has demonstrated that cobalamin binding pocket of cyanobacterial psB$_{12}$ accommodates the adenine of psB$_{12}$ in place of the DMB (Heal *et al.*, 2017). From this, we assume that MetH and psMe-B$_{12}$ have a 1:1 protein to cofactor.

Notably, the sample from HL 02 was the only one to have a ratio lower than 1:1 (HL 02 = 0.4 Me-psB$_{12}$: 1 MetH). This suggests that there was insufficient Me-psB$_{12}$ to occupy the MetH enzymes present. In contrast, HL 05.5 had 2.8 Me-psB$_{12}$:1 MetH. Both WH 8102 samples grown semi-continuously at 17 °C (low temp treatment) and environmental samples from HL 06 have close to the theoretical ratio of 1:1, indicating tight coupling of Me-psB$_{12}$ production and use in these samples. Cultures grown in batch had significantly more Me-psB$_{12}$ per cell than environmental samples and where therefore omitted from this graph but are displayed in Fig S4.

Discussion

Is protein abundance a suitable proxy for psB$_{12}$ quotas?

There is increasing interest in leveraging transcriptomic and proteomic data to infer rates and processes in microbial communities (Hawco *et al.*, 2020; Saito *et al.*, 2020; Roberts *et al.*, 2024) In theory, measuring coenzyme use (MetH) or production (CobO) could help approximate cellular concentrations or production rates of Me-psB$_{12}$. In practice, this requires a thorough understanding of psB$_{12}$ production, use, and changes in cofactor to protein ratios.

Here we show that CobO peptide per mol carbon did not always mirror psB$_{12}$ quotas. CobO abundance and psB$_{12}$ decreased in low temperatures but in stationary phase CobO was the lowest while Me-psB$_{12}$ was the highest (Fig 2). However, CobO is just one step of approximately 30 that are in the pathway to produce corrinoids de novo (Warren *et al.*, 2002). Contrary to what can be observed in many heterotrophic bacteria, Cob/Cbi genes in *Synechococcus* (including the strain used in this study, sp. 8102) are not clustered in operons and therefore may not be tightly co-regulated in *Synechococcus* (Rodionov *et al.*, 2003). The same environmental or physiological condition may thus have a different effect on different Cob/Cbi genes. Recent research determined that CobSV, CobQ and CobW are key genes that enhanced cobalamin synthesis in *Ensifer adhaerens* HY-1 when more highly expressed (Xu *et al.*, 2022). Future investigations into these genes, and others, may provide insight into the rate limiting step and regulation of psB$_{12}$ and B$_{12}$ biosynthesis.

MetH peptide abundance, perhaps a proxy for Me-psB$_{12}$ use, rarely followed the general variations we observed in Me-psB$_{12}$ in batch grown *Synechococcus* cultures. For example, in stationary phase MetH abundance was lowest while Me-psB$_{12}$ was highest (Fig 2B, F). In semi-continuously grown cultures, MetH was invariant while Me-psB$_{12}$ was significantly decreased in low N:P and temperature treatments (Fig 2C, G). However, the protein:co-factor stoichiometry for cultures grown at 17 °C were surprisingly close to 1:1, suggesting that under certain conditions inferring Me-psB$_{12}$ quota from MetH abundance may be reasonable (Fig 5C). Although neither MetH nor CobO abundance sufficiently estimated or corresponded to Me-psB$_{12}$ quota in cultured *Synechococcus* sp. 8102, the observed protein and co-factor variability still provides insight into psB$_{12}$-related cellular biology.

Variability in psB$_{12}$ quotas and protein inventories in Synechococcus cultures

The relationship between temperature and psB$_{12}$ production is particularly important when conceptualizing the spatio-temporal patterns psB$_{12}$ inventory and dynamics. Here, we demonstrate that 8102 grew significantly slower at 17 °C compared to the control 24 °C (Fig 2A, G), a result that is consistent with literature (Mackey *et al.*, 2015; Varkey *et al.*, 2016), and that Me-, OH-psB$_{12,}$ and CobO per mol carbon significantly decreased in low temperature (Fig 2B-I). Further investigation into the influence increased temperature has on psB$_{12}$ production, use and quota is an area of interest.

B$_{12}$ and nitrogen have been shown to co-limit productivity and influence community composition in various oceanic regions, including the coast of the Gulf of Alaska (Koch *et al.*, 2011), Long Island Embayment (Gobler *et al.*, 2007) and Eastern boundary of the South Atlantic gyre (Browning *et al.*, 2017). Here, we demonstrate that psB$_{12}$ quota in 8102 significantly decreased in low N:P, despite no change in growth rate or significant change in demand (MetH abundance) (Fig 2A, C). This result is of potential importance for the Scotian Shelf region, as a decrease in dissolved nitrogen relative to phosphorus has been observed since 2010 and is expected to continue in the future (Lehmann *et al.*, 2023). On average, the N:P ratio in

environmental samples was (3.5 ± 4.5 N:P) (Table S2) however no correlation between N:P and psB_{12} (pM) was observed. Further investigations of the relationships between N:P ratios, psB_{12} production, and remodeling activity are warranted.

Me-psB_{12} (nmol per mol carbon) was significantly higher in WH 8102 harvested at stationary phase compared to exponential phase (Fig 2B). In stationary phase, there were 20 Me-psB_{12} for every MetH, suggesting that there are significant pools of psB_{12} in cells that are not associated with MetH (Fig S3). This striking result points to either intracellular storage or alternative uses of Me-psB_{12} in *Synechococcus*, neither of which have been investigated in psB_{12} producers. Although roles for psB_{12} remain unknown, some alternative roles of B_{12} in the cell are beginning to be uncovered. For example, B_{12} is a sensitive light receptor and transcription regulator, albeit the benefit of these functions in stationary phase is not obvious (Ortiz-Guerrero *et al.*, 2011; Cheng *et al.*, 2016). Investigating the reservoirs of storage, accumulation, and alternative roles of psB_{12} could provide additional insight into the cellular processes that impact psB_{12} concentrations in cells and psB_{12} inventory in the ocean.

We observed a striking >350% increase of psB_{12} quota in cultures grown in batches compared to cultures grown semicontinuously (Fig 2B, C; Fig 6A). Interestingly, we observed the same influence of culture method when investigating B_{12} quota a recently isolated flavobacterium, *Pibocella* sp.. *Pibocella sp.* is a facultative B_{12} consumer, it does not make nor absolutely require B_{12}, but accumulates significantly more B_{12} per cell when grown in batch compared to semi-continuously – even at the same dissolved B_{12} concentration (Supplemental methods, Fig S4). Moreover, an increase in pgram B_{12} per µgram carbon was also observed when a haptophyte, *T. lueta,* was grown in batch cultures compared to in chemostats (Nef et al, 2019). The influence culture method has on both B_{12} and psB_{12} quota merits the question - *Which culture method best represents the regional, environmental conditions?*

Semi-continuous cultivation: most comparable to *in-situ* quotas

To determine which culture method best reflected psB_{12} dynamics in an environmental context, we compared the MetH to Me-psB_{12} stoichiometry from both culture and environmental studies. We found that samples from semi-continuously grown cultures most closely resembled the *in-situ* stoichiometry of *Synechococcus* communities in this region (Fig 5C). Semi-continuously grown cultures ranged from 1.2 to 8.2 Me-psB_{12} per MetH while environmental ranged from 0.4 to 2.8 Me-psB_{12} per MetH (Fig 5C). Batch grown cultures, although comparable to those reported in literature, had much greater psB_{12} concentrations than those measured in the environment (Fig S3). In this study, semi-continuously grown cultures appeared to be the most appropriate experimental approach for obtaining environmentally relevant data regarding psB_{12} in *Synechococcus* communities (Fig 5C). Comparing micronutrients quota between lab grown culture and environmental communities is rare but interest is growing. Our results highlight that careful consideration is required when trying to infer metabolite dynamics in the field through lab cultures.

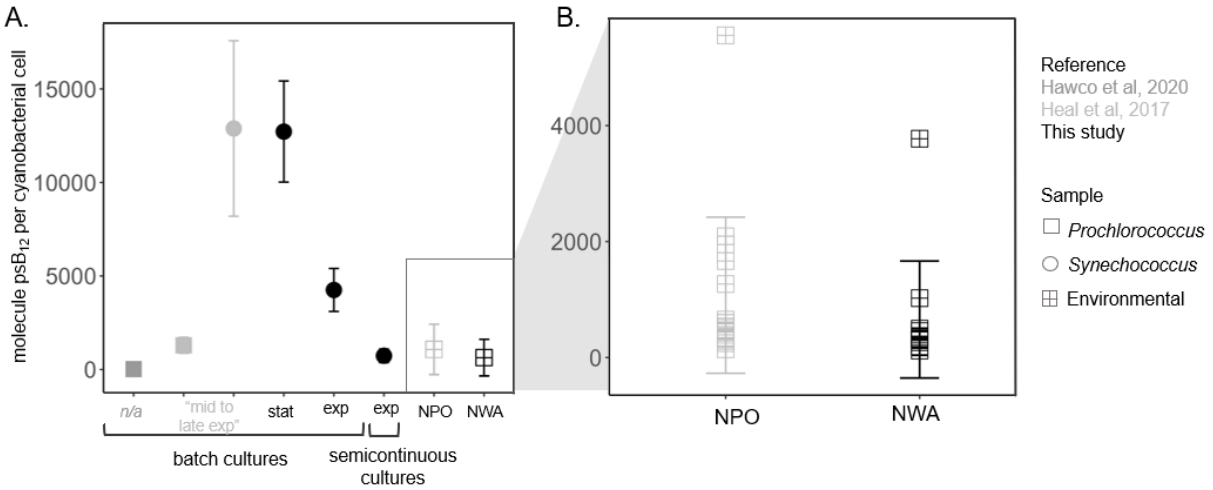

Figure 6: psB_{12} per cell in (A) cyanobacterial cultures and (B) the environment. (A) PsB_{12} per cell reported by Hawco et al, 2020* (dark gray), Heal et al, 2017 (light grey) and this study (black) in *Prochlorococcus* (square) and *Synechococcus* (circle) strains grown in batch or semicontinuously. Exp = exponential phase, stat = stationary phase. (B) psB_{12} quotas from Heal et al, 2017 from the North Pacific Ocean (NPO) (light grey) and from the Northwest Atlantic Ocean (NWA) (black) included in this study.
*psB_{12} was inferred from targeted proteomic measurements of MetH

Using cyanobacterial cell counts as a proxy for psB_{12} inventory

In this study, we provide the first set of environmental psB_{12} measurements in the Atlantic Ocean (Fig 3, 5). Here, psB_{12} accounted for 9 to 23% of total particulate cobalamin-related compounds (Fig7A, Table S2) - a significant part of total cobalamin that is missed if only B_{12} is measured. Missing psB_{12} measurements, especially in regions where cyanobacteria are abundant, restricts our ability to evaluate the importance psB_{12} and remodeling have on cobalamin production. However, measuring psB_{12}, like many marine metabolites, is inherently challenging due to low concentration in a complex matrix, and lack of commercially available standard (Moran *et al.*, 2022). Therefore, a proxy to estimate psB_{12} inventory could be a useful tool for researchers and further our understanding of when and how psB_{12} can influence marine microbial communities.

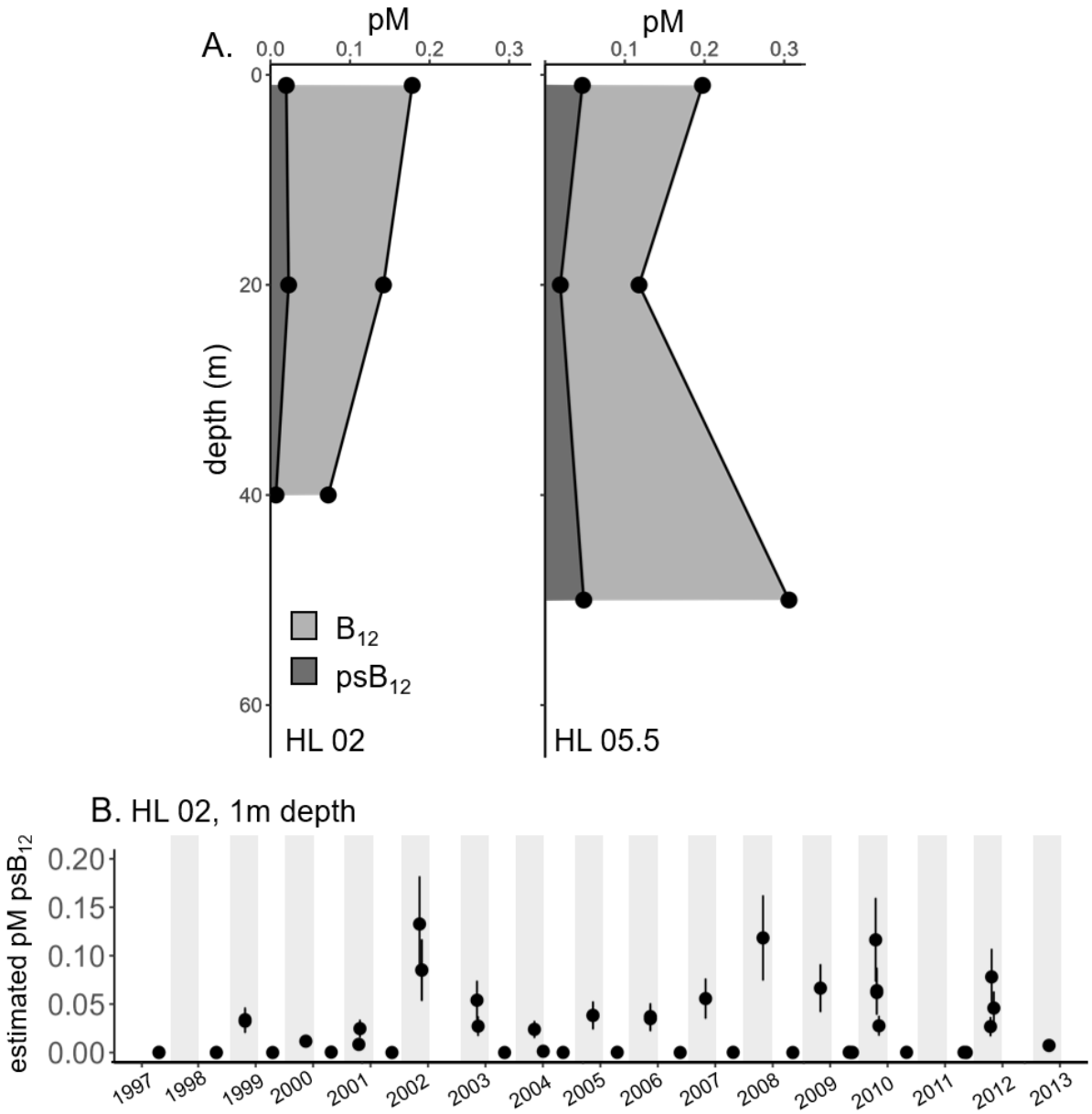

Figure 7: (A) psB_{12} (dark gray) and combined (light gray) total particulate B_{12} (pM) down the water column at HL 02 and HL 05.5. Environmental data presented in Table S2. (B) Estimated particulate psB_{12} inventory (pM) from 1997-2013 at HL 02 (1m) calculated from S*ynechococcus* cell counts provided by the Bedford Institute of Oceanography.

Here we found that 91% of our samples (10/11) contained 296 ± 101 Me-psB_{12} molecules per cyanobacteria cell (Fig 5A). The range of psB_{12} per cyanobacteria cell quantified in study was similar to the range of environmental measurements made from samples in the North Pacific Ocean (Heal *et al.*, 2017) (Fig 6B). The consistency of psB_{12} measured inspired us to consider whether cyanobacterial cell counts may be sufficient to predict psB_{12} inventory. For this case study, we estimated total psB_{12} inventory over years at station HL 02 based cyanobacterial cell counts from a historical dataset from the Bedford Institute of Oceanography (Fig 7B). While we used a narrower quota for this case study, we suggest that a general order of

485 10^3 psB_{12} molecules per cyanobacterial cell could be useful for estimating psB_{12} inventory from
486 cyanobacterial cell counts.

487 The 10^3 psB_{12} molecules per cyanobacterial cell estimate suggested here is *a* quota, not
488 *the* quota. Outliers from this range will undoubtedly appear with additional environmental
489 measurements. However, just like the outliers from HL 05.5, we believe that these outliers
490 provide valuable information that can guide future research. The value of psB_{12} per
491 cyanobacterial cell at 1 m from HL 05.5 still fall into a reasonable range reported by this study
492 and literature (Fig 6A, B) (Hawco et al, 2020; Heal et al, 2017) but there were outliers in our
493 samples (Fig 5C). HL 05.5 is located on the Scotian Shelf break, an oceanographically complex
494 region where the microbial community present is more diverse than other stations (Zorz *et al.*,
495 2019). Indeed, when examining the previously analyzed cyanobacterial (16S) mapped ASVs of
496 the samples used in this study, we see that samples from HL 05.5 had highest Shannon
497 diversity and chao values compared to the others sampled (Fig S6) (Robicheau *et al.*, 2022).
498 This indicates that community diversity may contribute to the increased Me-psB_{12} cell quota
499 seen in these samples – emphasizing the importance of psB_{12} measurements from a range of
500 cyanobacteria if more precise quota predictions are of utility.

501 ***Conclusion***

502 Although psB_{12} is a potentially significant source of B_{12} in the ocean, there are limited
503 measurements of it, and the factors that influence its production and use are unknown. Here, we
504 reveal that in culture conditions, psB_{12} quota decreases in low temperature and low N:P and that
505 both growth phase and culturing methods can impact psB_{12} quota. In samples from the
506 Northwest Atlantic Ocean, we found that psB_{12} quota per cyanobacteria cell was surprisingly
507 consistent. This provides researchers with a proxy to systematically incorporate cyanobacteria
508 and remodellers into conceptual and numerical models of environmental B_{12} dynamics by
509 estimating psB_{12} inventory. These quantitative values are a step towards understanding of the
510 role psB_{12} has in marine microbial communities.

511 **Acknowledgements**

512 Thanks Dr. Jenni Tolman for the advice on processing flow cytometry samples. We are grateful
513 to the Bedford Institute of Oceanography, Fisheries and Oceans Canada Atlantic Zone
514 Monitoring Program (AZMP) for access to the sea for the collection of samples analyzed in this
515 study. This study was funded by NSERC Discovery Grant RGPIN2015-05009 to EMB, Simons
516 Foundation Grant 504183 to EMB, Simons Foundation CBIOMES Award ID 1001702 to EMB,
517 Canada Research Chair Support to EMB, and NSERC CGS-D to CB.

518 **References**

519 Bertrand, E.M., McCrow, J.P., Moustafa, A., Zheng, H., McQuaid, J.B., Delmont, T.O., et al.
520 (2015) Phytoplankton–bacterial interactions mediate micronutrient colimitation at the
521 coastal Antarctic sea ice edge. *Proc Natl Acad Sci USA* **112**: 9938–9943.
522 Browning, T.J., Achterberg, E.P., Rapp, I., Engel, A., Bertrand, E.M., Tagliabue, A., and Moore,
523 C.M. (2017) Nutrient co-limitation at the boundary of an oceanic gyre. *Nature* **551**: 242–
524 246.
525 Cheng, Z., Yamamoto, H., and Bauer, C.E. (2016) Cobalamin's (Vitamin B12) Surprising
526 Function as a Photoreceptor. *Trends Biochem Sci* **41**: 647–650.
527 Dupont, C.L., Johnson, D.A., Phillippy, K., Paulsen, I.T., Brahamsha, B., and Palenik, B. (2012)
528 Genetic Identification of a High-Affinity Ni Transporter and the Transcriptional Response
529 to Ni Deprivation in Synechococcus sp. Strain WH8102. *Appl Environ Microbiol* **78**:
530 7822–7832.

Flombaum, P., Gallegos, J.L., Gordillo, R.A., Rincon, J., Zabala, L.L., Jiao, N., et al. (2013) Present and future global distributions of the marine Cyanobacteria Prochlorococcus and Synechococcus. *Proceedings of the National Academy of Sciences* **110**: 9824–9829.

Gleason, F.K. and Olszewski, N.E. (2002) Isolation of the Gene for the B12-Dependent Ribonucleotide Reductase from Anabaena sp. Strain PCC 7120 and Expression in Escherichia coli. *Journal of Bacteriology* **184**: 6544–6550.

Gobler, C., Norman, C., Panzeca, C., Taylor, G., and Sañudo-Wilhelmy, S. (2007) Effect of B-vitamins (B1, B12) and inorganic nutrients on algal bloom dynamics in a coastal ecosystem. *Aquat Microb Ecol* **49**: 181–194.

Gurdeep Singh, R., Tanca, A., Palomba, A., Van der Jeugt, F., Verschaffelt, P., Uzzau, S., et al. (2019) Unipept 4.0: Functional Analysis of Metaproteome Data. *J Proteome Res* **18**: 606–615.

Hawco, N.J., McIlvin, M.M., Bundy, R.M., Tagliabue, A., Goepfert, T.J., Moran, D.M., et al. (2020) Minimal cobalt metabolism in the marine cyanobacterium *Prochlorococcus*. *Proc Natl Acad Sci USA* **117**: 15740–15747.

Heal, K.R., Qin, W., Ribalet, F., Bertagnolli, A.D., Coyote-Maestas, W., Hmelo, L.R., et al. (2017) Two distinct pools of B_{12} analogs reveal community interdependencies in the ocean. *Proc Natl Acad Sci USA* **114**: 364–369.

Helliwell, K.E., Lawrence, A.D., Holzer, A., Kudahl, U.J., Sasso, S., Kräutler, B., et al. (2016) Cyanobacteria and Eukaryotic Algae Use Different Chemical Variants of Vitamin B12. *Current Biology* **26**: 999–1008.

Hoofnagle, A.N., Whiteaker, J.R., Carr, S.A., Kuhn, E., Liu, T., Massoni, S.A., et al. (2016) Recommendations for the Generation, Quantification, Storage, and Handling of Peptides Used for Mass Spectrometry–Based Assays. *Clinical Chemistry* **62**: 48–69.

Kido Soule, M.C., Longnecker, K., Johnson, W.M., and Kujawinski, E.B. (2015) Environmental metabolomics: Analytical strategies. *Marine Chemistry* **177**: 374–387.

Koch, F., Marcoval, M.A., Panzeca, C., Bruland, K.W., Sañudo-Wilhelmy, S.A., and Gobler, C.J. (2011) The effect of vitamin B12 on phytoplankton growth and community structure in the Gulf of Alaska. *Limnology and Oceanography* **56**: 1023–1034.

Koutmos, M., Datta, S., Pattridge, K.A., Smith, J.L., and Matthews, R.G. (2009) Insights into the reactivation of cobalamin-dependent methionine synthase. *Proceedings of the National Academy of Sciences* **106**: 18527–18532.

Lehmann, N., Reed, D.C., Buchwald, C., Lavoie, D., Yeats, P.A., Mei, Z.-P., et al. (2023) Decadal Variability in Subsurface Nutrient Availability on the Scotian Shelf Reflects Changes in the Northwest Atlantic Ocean. *Journal of Geophysical Research: Oceans* **128**: e2023JC019928.

Li, W.K.W. and Dickie, P.M. (2001) Monitoring phytoplankton, bacterioplankton, and virioplankton in a coastal inlet (Bedford Basin) by flow cytometry. *Cytometry* **44**: 236–246.

Li, W.K.W. and Wood, A.M. (1988) Vertical distribution of North Atlantic ultraphytoplankton: analysis by flow cytometry and epifluorescence microscopy. *Deep Sea Research Part A Oceanographic Research Papers* **35**: 1615–1638.

Loder, J., Han, G., Galbraith, P., Chasse, J., and van der Baaren, A. eds. (2013) Aspects of climate change in the Northwest Atlantic off Canada. *Canadian Technical Report of Fisheries and Aquatic Sciences 3045* 202.

Lu, X., Heal, K.R., Ingalls, A.E., Doxey, A.C., and Neufeld, J.D. (2020) Metagenomic and chemical characterization of soil cobalamin production. *ISME J* **14**: 53–66.

Lundin, D., Gribaldo, S., Torrents, E., Sjöberg, B.-M., and Poole, A.M. (2010) Ribonucleotide reduction - horizontal transfer of a required function spans all three domains. *BMC Evol Biol* **10**: 383.

Ma, A.T., Tyrell, B., and Beld, J. (2020) Specificity of cobamide remodeling, uptake and utilization in Vibrio cholerae. *Molecular Microbiology* **113**: 89–102.

Mackey, K.R.M., Post, A.F., McIlvin, M.R., Cutter, G.A., John, S.G., and Saito, M.A. (2015) Divergent responses of Atlantic coastal and oceanic Synechococcus to iron limitation. *Proc Natl Acad Sci U S A* **112**: 9944–9949.

Matthews, R.G., Koutmos, M., and Datta, S. (2008) Cobalamin-dependent and cobamide-dependent methyltransferases. *Current Opinion in Structural Biology* **18**: 658–666.

Moran, M.A., Link to external site, this link will open in a new window, Kujawinski, E.B., Link to external site, this link will open in a new window, Schroer, W.F., Link to external site, this link will open in a new window, et al. (2022) Microbial metabolites in the marine carbon cycle. *Nature Microbiology* **7**: 508–523.

Ortiz-Guerrero, J.M., Polanco, M.C., Murillo, F.J., Padmanabhan, S., and Elías-Arnanz, M. (2011) Light-dependent gene regulation by a coenzyme B $_{12}$ -based photoreceptor. *Proc Natl Acad Sci USA* **108**: 7565–7570.

Papadopoulos, J.S. and Agarwala, R. (2007) COBALT: constraint-based alignment tool for multiple protein sequences. *Bioinformatics* **23**: 1073–1079.

Roberts, M.E., Bhatia, M.P., Rowland, E., White, P.L., Waterman, S., Cavaco, M.A., et al. (2024) Rubisco in high Arctic tidewater glacier-marine systems: A new window into phytoplankton dynamics. *Limnology and Oceanography* **n/a**:

Robicheau, B.M., Tolman, J., Bertrand, E.M., and LaRoche, J. (2022) Highly-resolved interannual phytoplankton community dynamics of the coastal Northwest Atlantic. *ISME COMMUN* **2**: 1–12.

Rodionov, D.A., Vitreschak, A.G., Mironov, A.A., and Gelfand, M.S. (2003) Comparative Genomics of the Vitamin B $_{12}$ Metabolism and Regulation in Prokaryotes. *J Biol Chem* **278**: 41148–41159.

Saito, M.A., McIlvin, M.R., Moran, D.M., Santoro, A.E., Dupont, C.L., Rafter, P.A., et al. (2020) Abundant nitrite-oxidizing metalloenzymes in the mesopelagic zone of the tropical Pacific Ocean. *Nat Geosci* **13**: 355–362.

Soto, M.A., Desai, D., Bannon, C., LaRoche, J., and Bertrand, E.M. (2023) Cobalamin producers and prokaryotic consumers in the Northwest Atlantic. *Environmental Microbiology* **n/a**:

Suffridge, C.P., Gómez-Consarnau, L., Monteverde, D.R., Cutter, L., Arístegui, J., Alvarez-Salgado, X.A., et al. (2018) B Vitamins and Their Congeners as Potential Drivers of Microbial Community Composition in an Oligotrophic Marine Ecosystem. *Journal of Geophysical Research: Biogeosciences* **123**: 2890–2907.

Tanioka, Y., Miyamoto, E., Yabuta, Y., Ohnishi, K., Fujita, T., Yamaji, R., et al. (2010) Methyladeninylcobamide functions as the cofactor of methionine synthase in a Cyanobacterium, Spirulina platensis NIES-39. *FEBS Letters* **584**: 3223–3226.

Tanioka, Y., Yabuta, Y., Yamaji, R., Shigeoka, S., Nakano, Y., Watanabe, F., and Inui, H. (2009) Occurrence of Pseudovitamin B12 and Its Possible Function as the Cofactor of Cobalamin-Dependent Methionine Synthase in a Cyanobacterium Synechocystis sp. PCC6803. *J Nutr Sci Vitaminol* **55**: 518–521.

Varkey, D., Mazard, S., Ostrowski, M., Tetu, S.G., Haynes, P., and Paulsen, I.T. (2016) Effects of low temperature on tropical and temperate isolates of marine Synechococcus. *ISME J* **10**: 1252–1263.

Warren, M.J., Raux, E., Schubert, H.L., and Escalante-Semerena, J.C. (2002) The biosynthesis of adenosylcobalamin (vitamin B12). *Nat Prod Rep* **19**: 390–412.

Xu, S., Xiao, Z., Yu, S., Zeng, W., Zhu, Y., and Zhou, J. (2022) Enhanced cobalamin biosynthesis in Ensifer adhaerens by regulation of key genes with gradient promoters. *Synthetic and Systems Biotechnology* **7**: 941–948.

Zorz, J., Willis, C., Comeau, A.M., Langille, M.G.I., Johnson, C.L., Li, W.K.W., and LaRoche, J. (2019) Drivers of Regional Bacterial Community Structure and Diversity in the Northwest Atlantic Ocean. *Front Microbiol* **10**: 281.